IAA-AAS-DyCoSS2 -14-11-01

LIBRATION-POINT ORBIT MISSIONS DISPOSAL AT THE END-OF-LIFE THROUGH SOLAR RADIATION PRESSURE

Stefania Soldini,* Camilla Colombo,† Scott Walker,‡ and Markus Landgraf§ ¶

This paper investigates an end-of-life propellant-free disposal strategy for Libration-point orbits that allows the zero-velocity curves to be closed by exploiting solar radiation pressure. The spacecraft is initially disposed into the unstable manifold leaving the Libration-point orbit, before a reflective sun-pointing surface is deployed to enhance the effect of solar radiation pressure. Therefore, the consequent increase in energy prevents the spacecraft's return to Earth. An energetic approach is used to compute the required area for the Hill's curve closure at the pseudo Libration-point SL_2, via numerical optimisation. Three European Space Agency missions are selected as test case scenarios: Herschel, SOHO and Gaia. Finally, guidelines for the end-of-life disposal of future Libration-point orbit missions are proposed.

INTRODUCTION

Libration-Point Orbit (LPO) missions are often selected for studying the Sun and the Universe. Example missions include SOHO, which studies the Sun's outer corona and the solar wind, and Herschel, which investigates the formation of galaxies. The European Space Agency (ESA) just succeeded in launching a space telescope with the Gaia mission, while NASA's James Webb Space Telescope will provide astronomical data to understand the formation of galaxies, stars, planets and life, and Euclid will map the geometry of the dark Universe. Orbits around the Libration-points L_1 and L_2 of the Sun-Earth system are advantageous as they can reached from the Earth and, since a constant geometry is ensured with respect to the Sun and Earth, they are used for space observation with advantages in the ease of communication to the Earth and in thermal system design. However, they lie in highly perturbed regions; therefore, an uncontrolled spacecraft would naturally follow the unstable manifold and after several years could cross the protected regions at the Earth and the L_1/L_2 regions. In addition, since LPO's spacecraft are characterised by large dry masses, it is critical to clear these regions once the mission has ended.

This paper proposes an End-Of-Life (EOL) disposal option towards the outer part of the Earth-Sun system exploiting Solar Radiation Pressure (SRP). This strategy was developed as part of an ESA study on EOL disposal concepts for Lagrange-Point and Highly Elliptical Orbit Missions.[1] Olikara et al.[2] previously proposed a disposal option, which injects the spacecraft towards the inner or the outer solar system and closes the Hill's surfaces though a Δv manoeuvre. In this article, an alternative disposal strategy is investigated that allows the closure of the zero-velocity curves by means of SRP. In this case, the spacecraft is disposed at the EOL onto the unstable manifold leaving the LPO from L_2. Then, a SRP-enhancing device is deployed to close the curves and, thus, prevent the spacecraft's return to the Earth and protect the L_2 region. This strategy can be achieved through a sun-pointing auto-stabilised deployable structure, such as light reflective surfaces which are already proven for attitude control applications (*e.g.*, GOSE's solar sail[3]), with the advantage of saving propellant.

*PhD Candidate, Astronautics Research Group, University of Southampton, Southampton, UK, s.soldini@soton.ac.uk.
†Lecturer, Astronautics Research Group, University of Southampton, currently, Marie Curie Research Fellow at Politecnico di Milano, Milan, Italy, camilla.colombo@polimi.it.
‡Lecturer, Astronautics Research Group, University of Southampton, Southampton, UK, sjiw@soton.ac.uk.
§Mission Analyst, ESA/ESOC, Darmstadt, Germany, markus.landgraf@esa.int.

In this article an energetic approach is used to close the Hill's curves at SL_2 (*e.g.*, the pseudo Libration-point L_2 when SRP is added[4]) by increasing the energy of the system and then computing the reflective deployable area required for the EOL curves-closure. As a term due to SRP is added to the energy, the shape of the potential surfaces changes and the required reflective area is computed via numerical optimisation, imposing the condition for curves closures, that is, the augmented energy equals the energy at SL_2. After the closure, the spacecraft is bounded in its following motion at the right side of the pseudo point to guarantee that the spacecraft squared velocity is positive. It is also demonstrated that the spacecraft cannot be confined towards the inner solar system and that the disposal through SRP can only be performed at SL_2.

Three ESA missions are selected as scenarios: Herschel, SOHO and Gaia. Results show that the area required is lower if the deployment is performed further away from the Sun. Moreover, higher initial energy requires a larger deployed area at a fixed distance from the Sun. A preliminary discussion is presented on the effect on the Earth's eccentricity on the disposal strategy. Finally, guidelines for the EOL of future LPO missions are proposed. Through this strategy, the existing structures on-board the spacecraft can be exploited by deploying an additional area such as solar panel flaps or a modified sunshield geometry.

DYNAMICAL MODEL

The spacecraft's motion is described in the Circular Restricted Three-Body Problem (CRTBP) and the effect of the SRP (CRTBPS) is included into the dynamics at the moment of the zero-velocity curves closure at SL_2.[4,5] The Elliptic Restricted Three-Body Problem with SRP (ERTBPS) dynamics are also shown here since it will used to preliminary discuss the Earth's eccentricity effect.[6,7] Indeed, small perturbations in the CRTBPS may prevent the curve closure.

Circular Restricted-Three Body Problem with Solar radiation pressure (CRTBPS)

The dynamics are written in the non-dimensional rotating coordinate frame (synodic system, Figure 1):[8]

$$\begin{cases} \ddot{x} - 2\omega\dot{y} = -\bar{U}_x(x,y,z) + U_{s_x}(x,y,z,\beta) \\ \ddot{y} + 2\omega\dot{x} = -\bar{U}_y(x,y,z) + U_{s_y}(x,y,z,\beta) \\ \ddot{z} = -\bar{U}_z(x,y,z) + U_{s_z}(x,y,z,\beta) \end{cases} \tag{1}$$

where, $\bar{U}(x,y,z)$ is the total potential which includes the contribution of the rotating system potential $U_r(x,y)$ and the gravitational potential $U_g(x,y,z)$.

$$\bar{U}(x,y,z) = U_r(x,y) + U_g(x,y,z) \tag{2}$$

The rotating potential is:

$$U_r(x,y) = -\frac{1}{2}(x^2+y^2) \tag{3}$$

and the gravitational potential is:

$$U_g(x,y,z) = -\frac{\mu_{Sun}}{r_{Sun-p}} - \frac{\mu_{Earth}}{r_{Earth-p}} \tag{4}$$

In Eqs. (4), r_{Sun-p} and $r_{Earth-p}$ are, respectively, the spacecraft's distance from the Sun and the Earth:

$$r_{Sun-p} = \sqrt{(x-x_{Sun})^2+y^2+z^2} \tag{5}$$

$$r_{Earth-p} = \sqrt{(x-x_{Earth})^2+y^2+z^2} \tag{6}$$

In non-dimensional coordinates, $x_{Sun} = -\mu$ is the position of the Sun and $x_{Earth} = 1-\mu$ is the position of the Earth-Moon barycentre. The primaries unit masses are defined as $\mu_{Earth} = \mu$ and $\mu_{Sun} = 1-\mu$ where, $\mu = \frac{m_{Earth}}{M_{Sun}+m_{Earth}}$ is the mass parameter of the Sun-(Earth-Moon) system, equal to $3.04042 \cdot 10^{-6}$. In non-dimensional coordinates the angular velocity of the synodic system at the barycentre ω is the mean motion ad it is equal to 1.

The SRP model used in this study is the cannonball model, which gives a first approximation of the solar radiation effect when included in the RTBP dynamics. The advantage of using the cannonball model is in the possibility of expressing the SRP force as a potential function for a Sun-pointing reflective surface, which makes it easy to analytically investigate the perturbation effect using the Lagrange approach. Therefore, for a Sun-pointing reflective surface (with δ equal to zero, Figure 1), the potential of SRP forces is:

$$U_s = \beta \frac{\mu_{Sun}}{r_{Sun-p}} \tag{7}$$

In Eq. (7), $\beta = \frac{\sigma^*}{\sigma}$ is the lightness parameter and it is a function of the area-to-mass ratio and the Sun luminosity as $\sigma = \frac{m}{A}$ and $\sigma^* = \frac{L_{Sun}}{2\pi c \mu_{Sun}} = 1.53$ [g/m^2] [5] for the specific case where the reflectivity coefficient (C_r) is 2. Moreover, β is defined within the range of 0 (no SRP effect) and 1 (SRP counteracts the gravitational effect of the Sun).

One of the aims of this study is also to investigate if it is necessary to use specifically designed deployable reflective area for disposal or if it is possible to exploit some existing reflective deployable areas and then, at the EOL, change their original configuration for the zero-velocity closure.

Elliptic Restricted-Three Body Problem with Solar radiation pressure (ERTBPS)

Once the requirements for the zero-velocity curves closure are defined, it is of interest to verify how the effect of the Earth's eccentricity affects the area needed for the closure. The dynamics of the ERTBPS for a sun-pointing reflective surface is written in a non-uniformly, non-dimensional, rotating and pulsating reference frame:[6,7]

$$\begin{cases} x'' - 2y' = \omega_x \\ y'' + 2x' = \omega_y \\ z'' = \omega_z \end{cases} \tag{8}$$

where, ω is the potential function of the system and it is defined as:

$$\omega = \frac{\Omega}{1 + e cos(f)} \tag{9}$$

with Ω as:

$$\Omega = \Omega' - \frac{1}{2}(1 + e cos(f)) z^2 \tag{10}$$

$$\Omega' = \frac{1}{2}(x^2 + y^2 + z^2) + (1 - \beta)\frac{\mu_{Sun}}{r_{Sun-p}} + \frac{\mu_{Earth-p}}{r_{Earth-p}} \tag{11}$$

In Eq. (8), f is the true anomaly, e is the eccentricity of the primaries when their dynamics is described in the two-body problem. The symbol [$'$] denotes the derivation with respect to the true anomaly (i.e., pulsating coordinate). The definition of r_{Sun-p} and $r_{Earth-p}$ is the same of Eq. (5) and Eq. (6) respectively.

ENERGY APPROACH

The spacecraft is supposed to have a deployable EOL device, to close the zero velocity curves at SL_2 after its deployment. This device is configured to be Sun-pointing, so the SRP force admits a potential form and auto-stabilised.[9] The same formulation was analysed in two different cases: the first one when the effect of SRP is taken into account only after the deployment in the CRTBPS and the second one when the effect of SRP is considered after the injection into the manifold and then the minimum area required is computed as a delta SRP effect in the CRTBPS due to, as for example, the deployment of reflective flaps from the original spacecraft sunshade configuration. In this paper, only the second case is discussed because including the SRP

from the manifolds injection influences the manifolds evolutions (i.e., small perturbations in the position), while the required reflective area for the disposal is very similar in the two cases.

In the CRTBPS the total potential U has the contribution of the rotating system potential plus the gravitational potential, $\bar{U}$ (Eq. (2)) and the solar radiation pressure potential U_s (Eq. (7)). In the rotating frame with non-dimensional coordinates it assumes the form:

$$U(x, y, z, \beta_0) = \bar{U}(x, y, z) + U_s(x, y, z, \beta_0) \tag{12}$$

where, β_0 is given by the effect of the spacecraft's initial dry area-to-mass ratio.

The energy with the effect of the spacecraft's initial dry area-to-mass ratio is defined as:

$$E(x, y, z, \dot{x}, \dot{y}, \dot{z}, \beta_0) = \bar{E}(x, y, z, \dot{x}, \dot{y}, \dot{z}) + U_s(x, y, z, \beta_0) \tag{13}$$

where,

$$\bar{E}(x, y, z, \dot{x}, \dot{y}, \dot{z}) = \frac{1}{2}(\dot{x}^2 + \dot{y}^2 + \dot{y}^2) + \bar{U}(x, y, z) \tag{14}$$

When a near-perfect reflective flap is deployed, the energy increases to:

$$E(x, y, z, \dot{x}, \dot{y}, \dot{z}, \beta_0, \Delta\beta) = \bar{E}(x, y, z, \dot{x}, \dot{y}, \dot{z}) + U_s(x, y, z, \beta_0) + U_s(x, y, z, \Delta\beta) \tag{15}$$

By expressing all the terms in Eq. (15), it can be rewritten as:

$$E(\boldsymbol{X}, \beta_0, \Delta\beta) = \frac{1}{2}V^2 - \frac{1}{2}(x^2 + y^2) - (1 - \beta_0)\frac{\mu_{Sun}}{r_{Sun-p}} - \frac{\mu_{Earth}}{r_{Earth-p}} + \Delta\beta\frac{\mu_{Sun}}{r_{Sun-p}} \tag{16}$$

V is the magnitude of the spacecraft velocity $\{\dot{x}, \dot{y}, \dot{z}\}$ along the manifolds computed in the CRTBPS (before the closure $\beta = \beta_0$, in Eq. (1)).

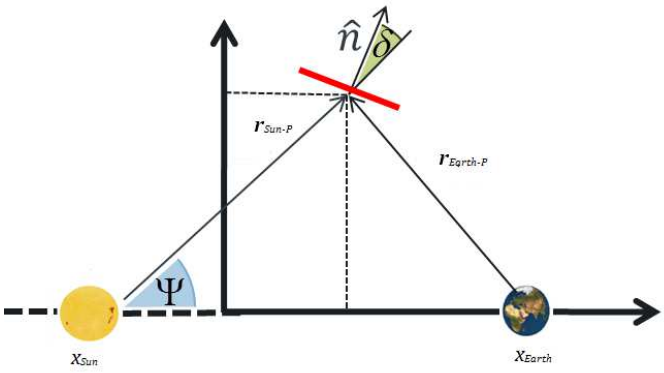

Figure 1: Planar circular restricted three-body problem: rotating frame.

In order to find the minimum area required to close the zero velocity curves at SL_1 or SL_2, it is necessary to satisfy the following constraint:

$$E(\boldsymbol{X}_{SL_j}, \beta_0, \Delta\beta_{min}) = E(\boldsymbol{X}_{P_1}, \beta_0, \Delta\beta_{min}) \tag{17}$$

where, $\boldsymbol{X}_{SL_j} = \{x_{SL_j}, 0, 0, 0, 0, 0\}$ is the position of the Lagrange point with SRP, Eq. (17) can be written as:

$$\begin{aligned} \tfrac{1}{2}V_{P_1}^2 = \; & \tfrac{1}{2}(x_{P_1}^2 + y_{P_1}^2 - x_{SL_j}^2) - \mu_{Sun}(1 - \beta_0)\left[\tfrac{1}{r_{Sun-SL_j}} - \tfrac{1}{r_{Sun-P_1}}\right] - \mu_{Earth}\left[\tfrac{1}{r_{Earth-SL_j}} + \right. \\ & \left. - \tfrac{1}{r_{Earth-P_1}}\right] + \mu_{Sun}\Delta\beta\left[\tfrac{1}{r_{Sun-SL_j}} - \tfrac{1}{r_{Sun-P_1}}\right] \end{aligned} \tag{18}$$

where the index "j" refers to the location (either SL_1 or SL_2) where the closure occurs.

From the numerical point of view the boundaries of $\Delta\beta$ required during the optimisation are 0 and 1-β_0.

If we now focus on a planar motion with $\beta_0 = 0$, therefore $\beta = \beta_0 + \Delta\beta = \Delta\beta$, Eq. (18) can be simplified as:

$$\frac{1}{2}V_{P_1}^2 = \frac{1}{2}(x_{P_1}^2 + y_{P_1}^2 - x_{SL_j}^2) - \mu_{Sun}(1-\beta)\left[\frac{1}{r_{Sun-SL_j}} - \frac{1}{r_{Sun-P_1}}\right] - \mu_{Earth}\left[\frac{1}{r_{Earth-SL_j}} - \frac{1}{r_{Earth-P_1}}\right] \tag{19}$$

For simplicity a state vector P_1 which has only one non zero component in the x-direction and a velocity magnitude which respects the conservation of the energy has been considered. It is possible to investigate when the energy intersection, in Eq. (17) is feasible for the zero velocity closure in SL_j. Figure 2 and Figure 3 displays the right (i.e., coloured line) and the left (i.e., black line) side of Eq. (17) evaluated at SL_1 and SL_2, respectively. As it can be seen, a feasible solution does not always exist which allows the Hill's curves to be closed. This is evident in Figure 2 for the solution x = 0.65 (blue line). Indeed, β is constrained within 0 and 1, so the value of the increased energy is constrained (see Table 1). Finally, it is interesting to note that a lower β is required when closing in SL_2 by comparing Figure 2 and Figure 3.

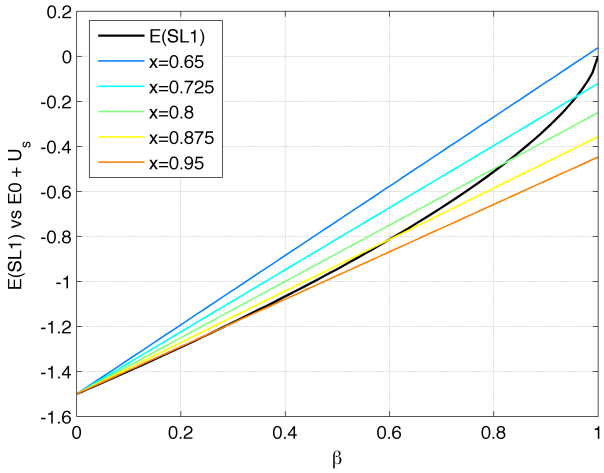

Figure 2: Intersection with $E(x_{SL_1}, \beta)$ and right side of Eq. (17) in correspondence of SL_1.

In order to achieve the closure at SL_j, it is necessary to satisfy Eq. (19). The left side of Eq. (19) contains the squared velocity for a generic point P_1, which is a positive term. Therefore, if we study the sign of all the terms in Eq. (19), we have to demonstrate that the expression on the left side is positive ($V_{P_1}^2 > 0$). In this paper, only the case in which P_1 is between the Earth and SL_2 region is shown (see Figure 4); however, it can be easily demonstrated that we would achieve the same results if P_1 is one of the gray points in Figure 4. For the case shown in Figure 4, the condition of $V_{P_1}^2 > 0$ can be guaranteed only if P_1 stays at the right side of, as an example, SL_1. In this way, the first term on the right side of Eq. (19) is a positive term. Instead, r_{Sun-SL_1} is less than r_{Sun-P_1} in modulus and they are both positive in magnitude. Therefore, the second term on the right side is negative. Moreover, $r_{Earth-SL_1}$ is bigger than $r_{Earth-P_1}$ in magnitude and they are both positive. Therefore, the third term on the right is positive. Finally, the first term on the right side is bigger than the second plus the third term, so this condition is satisfied only if P_1 is at the right side of SL_1. Conversely, in case of SL_2 the second and the third terms of the right side of the equation are both positive. However, the squared distance of SL_2 from the center of mass is bigger then the projected squared distance of P_1 in the x-y plane with respect to the center of mass. Thus, the first term on the right side is now negative and, in order to achieve a positive squared velocity after the closure, P_1 should stays on the

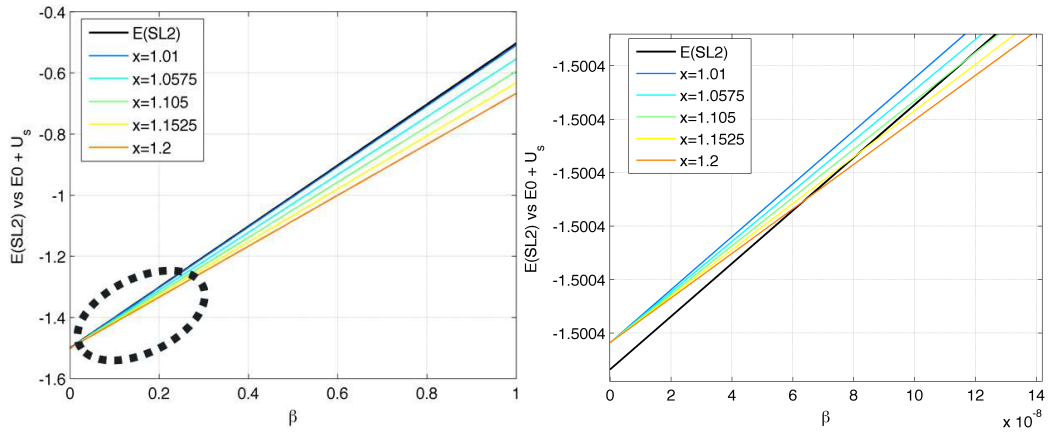

(a) (b)

Figure 3: Intersection with $E(x_{SL_2}, \beta)$ and right side of Eq. (17) in correspondence of SL_2.

right side of SL_2. This can be demonstrated also when P_1 corresponds to the gray points in Figure 4. This condition is necessary, but not sufficient to find β that closes the zero-velocity curves since there are some cases where a solution does not exist. Ultimately, it is interesting to note that, when the velocity in P_1 is zero, P_1 is coincident to SL_j.

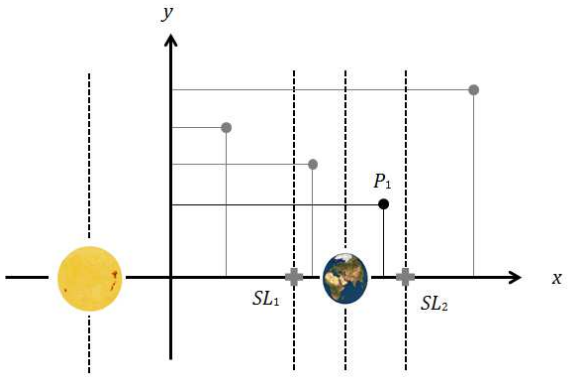

Figure 4: Reference system for studying the clousure in SL_j.

Table 1: Positions of L_1 and L_2 as a function of SRP.

β	x_{L_1}	x_{L_2}
0	0.989985982354727	1.010075200010617
1	$-0.105864912811615 \cdot 10^{-4}$	1.001739126300185

In order to understand the effect of the Earth's eccentricity on the disposal strategy, it is necessary to introduce the equation of the energy in the ERTBP[10] with SRP (ERTBPS) which is:

$$x'^2 + y'^2 + z'^2 = 2\omega - 2e\int_0^f \frac{\Omega sin(f)}{(1+ecos(f))^2}df - e\int_0^f \frac{z^2 sin(f)}{1+ecos(f)}df - C \tag{20}$$

where ω is defined as in Eq. (9) and C is the Jacoby constant. When the true anomaly identifies the perigee ($f = \bar{f} = 0$) and the apogee ($f = \bar{f} = \pi$), Eq. (20) turns into Eq. (21), since $sin(\bar{f}) = 0$ the two integrals vanish.

$$x'^2 + y'^2 + z'^2 = 2\bar{\omega} - C \tag{21}$$

In Eq. (21), C is equal to $-2E$ and $\bar{\omega}$ is a function of $\bar{f}$ and can be written as:

$$\bar{\omega} = \frac{1}{(1+ecos(\bar{f}))}\left[\frac{1}{2}(x^2+y^2+z^2) + (1-\beta)\frac{\mu_{Sun}}{r_{Sun-p}} + \frac{\mu_{Earth}}{r_{Earth-p}}\right] - \frac{1}{2}z^2 \tag{22}$$

STRATEGY DESCRIPTION

To design a strategy that enables the solar radiation pressure to be used to close the zero velocity curves at SL_2, we need to compute the unstable manifold towards the outer system. The unstable manifold is computed by integrating forward in time with a perturbation of $+\epsilon = 10^{-6}$ which corresponds to a displacement error in the spacecraft position of $D = 200$ km.[11,12] A number of trajectories which belong to this unstable tube (Figure 5a) are selected with their initial condition close to the LPO. Then, a series of points P_1 along each natural trajectory legs are selected (Figure 5b), where a sun-pointing reflective surface is deployed (Figure 5c). This allows the closure of the zero velocity curves at SL_2. The trajectories evolution after the deployment was verified, computing the new trajectory legs by adding the effect of β (Figure 5d). It can be verified that, in correspondence of any point P_2 of the following evolution, the zero velocities curves are closed (see Figure 5) since the energy does not change. In this way, the energy of the system was changed without any propellant costs. It is interesting to note that, with respect to the strategy proposed by Olikara et al.,[2] here the energy is increased rather than decreased.

Figure 6 shows an example of the SRP disposal strategy for a two dimensional case. The time used for the manifold evolution is about 400 non-dimensional time units; which corresponds to 63.5 years. As can be seen from Figure 6a, the strategy to inject the spacecraft towards the unstable manifolds without providing any Δv to close the zero velocity curves is unsafe because of the creation of potential space debris in LPO, hence this approach is not sustainable. Indeed, the highlighted trajectory in Figure 6a (red line) shows that after 63.5 years the spacecraft, which was previously disposed to the unstable manifold, will encounter the Earth and L_2 regions since the zero-velocity curves have a trajectory gateway in L_2. Instead, after the EOL device is deployed (Figure 6b), the zero velocity curve can be closed (Figure 6c). Finally, even if the L_2 region is not completely protected (Figure 6d), the probability of crossing close to L_2 is now lower.

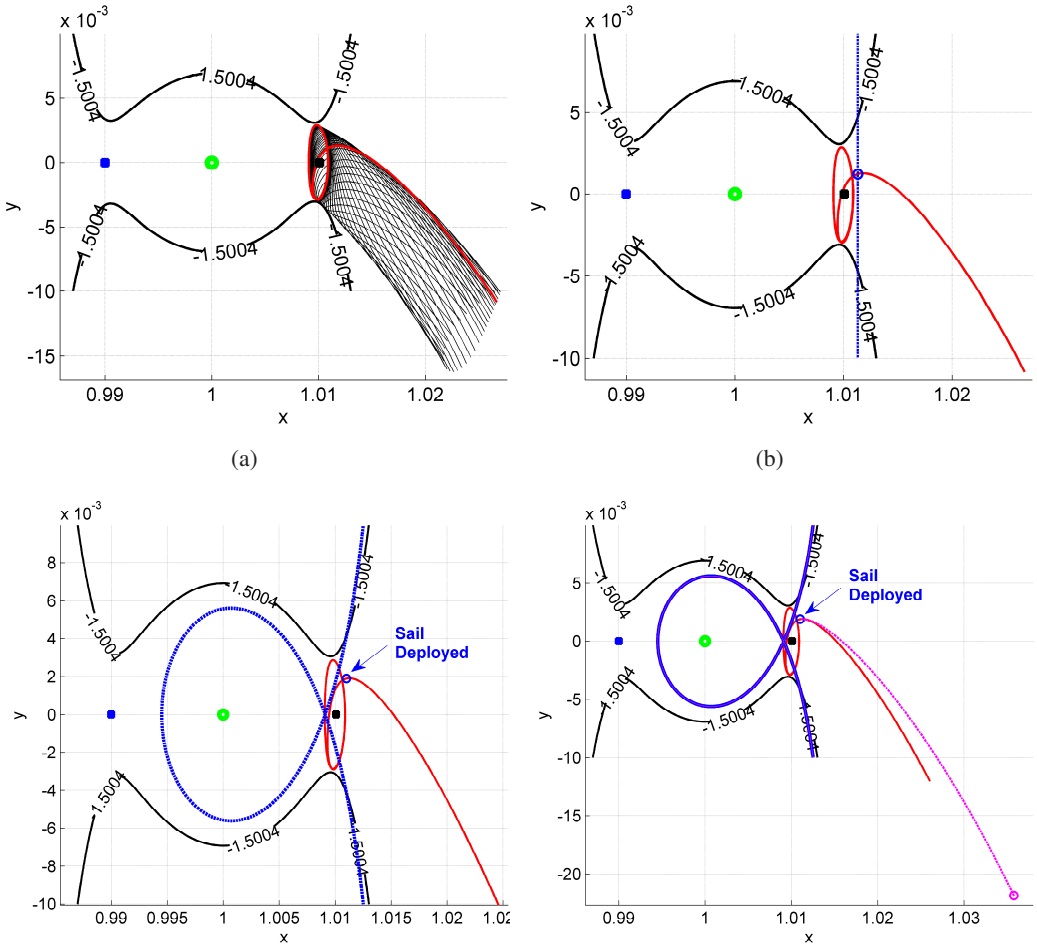

Figure 5: End-of-life disposal sequence after 68.04 days of manifold injection.

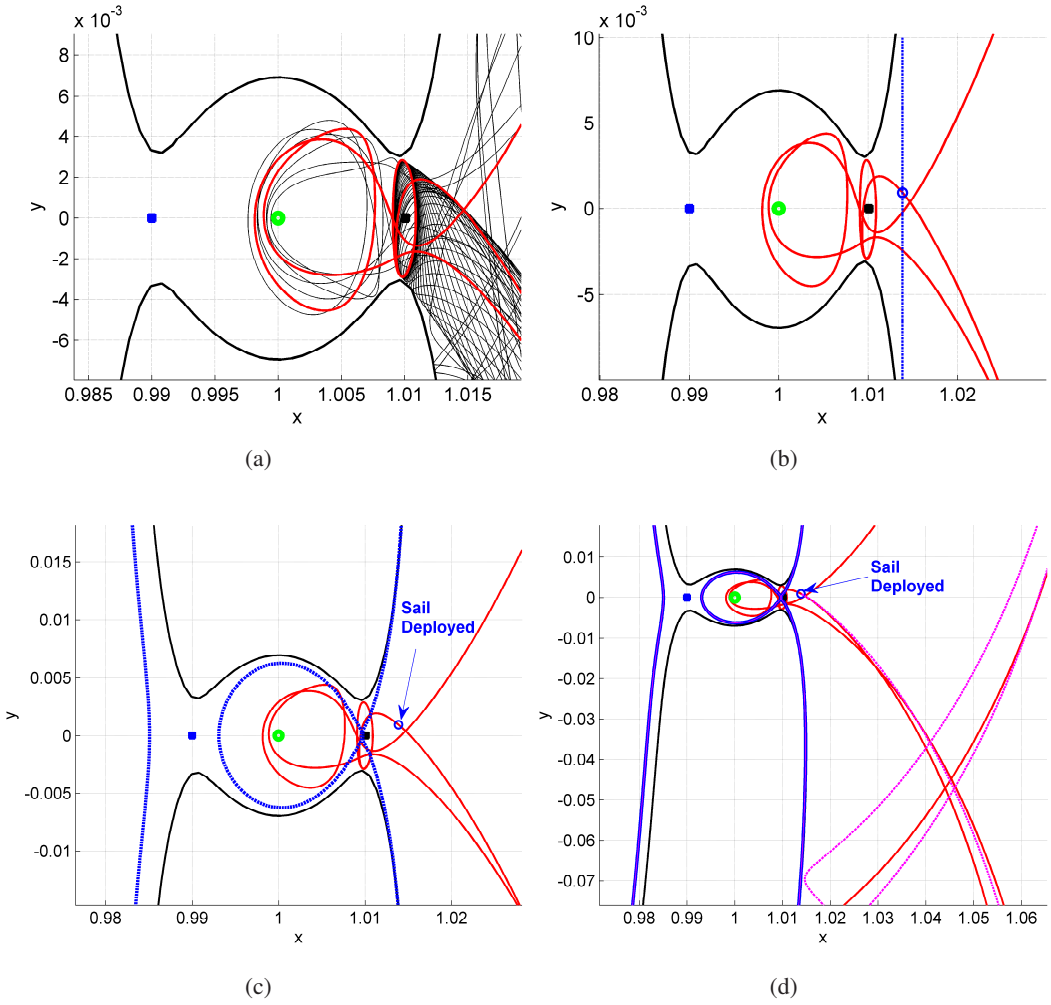

Figure 6: End-of-life disposal sequence after 68.04 days of manifold injection with 63.5 years of trajectory evolution.

Effect of the Earth's eccentricity

A preliminary study to understand the effect of the Earth's eccentricity onto the proposed disposal strategy has been performed. Due to the non-autonomous nature of the ERTBP, the dynamics does not allow the use of the Jacobian integral any more. Consequently, the effect of the Earth's eccentricity on the zero-velocity curves has been analysed at the perigee and apogee. The cases illustrated in Figure 7 and Figure 8 are linked to the sequences shown in Figure 6. The EOL area that closed the zero-velocity curves was initially calculated using the CRTBP (and is shown as a blue circle in Figure 6d). This condition was used as a basis for the ERTBPS study at the perigee and apogee. To avoid discontinuity in the position vector, the same position was maintained for the two cases in the ERTBPS. Moreover, it has been supposed to maintain the same initial energy that represent the motion in the CRTBPS. Therefore, it has been computed the magnitude of the velocity vectors in the ERTBS at the perigee and apogee by inverting Eq. (21). In Figure 7a, the zero-velocity curves closure after the deployment in the CRTBPS (blue and magenta lines) and in the ERTBPS at the perigee (green line) is shown. It is possible to notice that the trajectory evolution of the CRTBPS (red line) is completely contained within the forbidden region of the ERTBPS at the perigee (defined by the green lines in Figure 7a). Therefore, it is not possible, in this case, to integrate the dynamics in the ERTBPS after the deployment, but this may suggest that the area computed in the CRTBP is enough to guarantee a safe closer in the real case. Instead, Figure 7b shows that at the apogee there is no forbidden region (if the energy of the system is the same as the CRTBPS case); therefore, the motion is always permitted. The black dash line is representative of the spacecraft trajectory evolution if, after the deployment, the dynamical model is in the ERTBPS and started at the apogee. This simulation is representative of 63.5 years in the CRTBPS (see red line in Figure 7a) and 25 years for the ERTBPS dynamics at the apogee (see black dash line in Figure 7b). Finally, Figure 8a and Figure 8b compares the dynamics in the CRTBP and in the ERTBP at the apogee for two cases. The first when no structure is deployed and therefore the zero-velocity curves remain open (Figure 8a) and the second for the case when a SRP enhancing device is deployed at the blue circle (Figure 8b). For both cases the dynamics in the ERTBP or ERTBPS at the apogee are studied for 63.5 years. The effect of the structural deployment is that the trajectory of the spacecraft drifts in such a way that after 63.5 years it does not cross the L_1- Earth-L_2 regions. However, this does not prove that the deployment of a SRP enhancing device will always achieve this condition for another selected trajectory along the unstable manifolds. It therefore remains an area which is under investigation. Additionally, since the motion is unrestricted and can cross the L_1- Earth-L_2 regions, statistically this will occur if the simulation time is increased. To explore this problem in greater depth a full analysis using the ERTBPS needs to be performed. This is an area of future research.

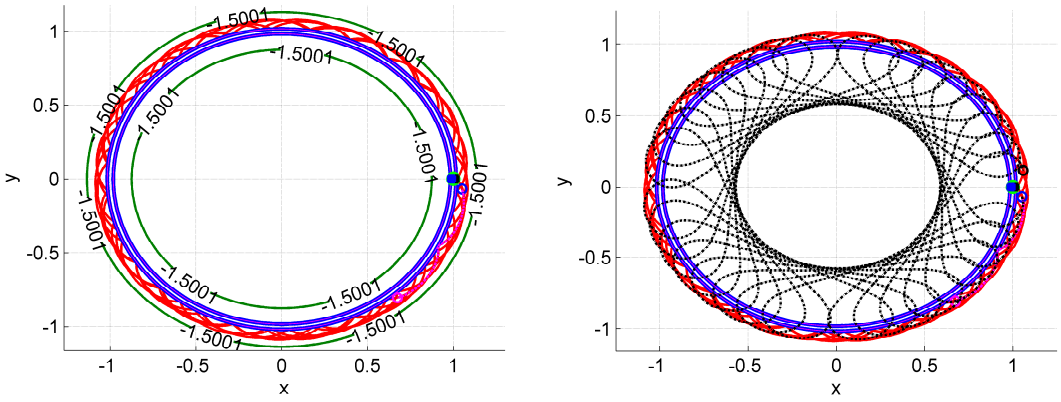

(a) Zero-velocity curves in the ERTBPS (green line) at the perigee

(b) Zero-velocity curves in the ERTBPS (no forbidden region) at the apogee within 25 years.

Figure 7: Comparison with the planar dynamics in the CRTBPS and the ERTBPS.

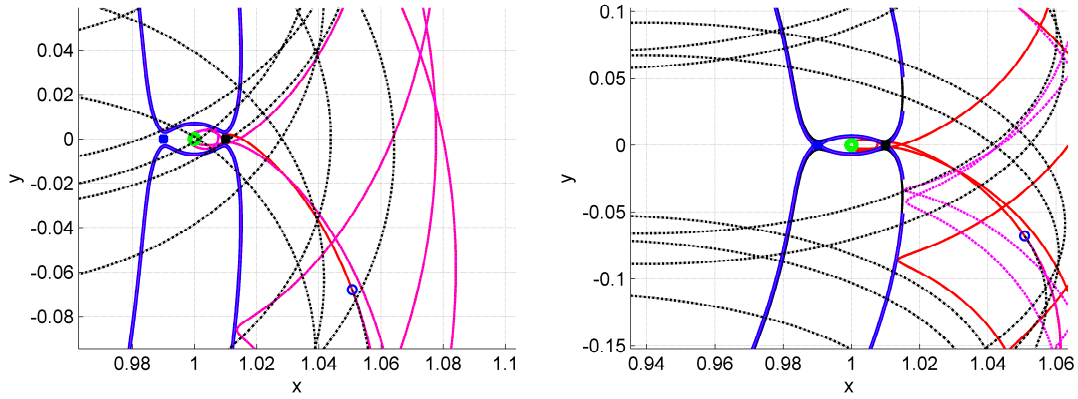

(a) Dynamics without SRP: CRTBP (red and magenta) and ERTBP (black dash line) at apogee within 63.5 years.

(b) Dynamics with SRP: CRTBP (red), CRTBPS (magenta) and ERTBPS (black dash line) at apogee within 63.5 years.

Figure 8: Comparison with the planar dynamics in the ERTBP at the apogee with and without SRP.

END-OF-LIFE DISPOSAL OF LPO MISSIONS

LPO spacecraft were historically placed in halo orbits at L_1 to study the Solar wind in the Sun-Earth system, and in L_1 and L_2 in the Earth-Moon system to study the Earth's magnetotail. The majority of these missions are in a Lissajous orbit either at L_1 and L_2. Instead, future LPO missions will be placed in the Sun-Earth system with a major interest in L_2 missions for next generation space telescopes. A literature search was performed to characterise current, past and future ESA LPO missions, in terms of LPO amplitude and spacecraft characteristics. The halo orbits selected by past ESA missions have an amplitude from 200,000 to 300,000 km, 500,000 to 800,000 km and 120,000 to 10^6 km in A_x, A_y and A_z respectively. Instead, the Lissajous orbits have amplitude from 340,000 to 750,000 km and 90,000 to 450,000 km in A_y and A_z respectively. The area-to-mass (dry) of the ESA's LPO spacecraft is between 0.004 to 0.06 m^2/kg, which is close to the EOL area-to-mass (wet) value since the fuel mass percentage is very low. It can also be noted that future missions show the tendency to choose higher amplitude orbits for both halo and Lissajous orbits. Three LPO missions selected for this study are presented in this section: Herschel,[13] SOHO[14] and Gaia.[15] The overall cross section area used to compute the area-to-mass ratio was found by considering the spacecraft spin axis constraints, when applicable. In the case of missions around L_1, the projected areas are the spacecraft solar array and the spacecraft bus. On the other hand, for missions around L_2 the projected areas are the spacecraft sunshade and the solar array. Note that the values shown for disposal towards the outer solar system through SRP are for the exact closure of the velocity curves; in reality, a margin on those required areas should be added to ensure that the trajectory cannot return to Earth due to perturbations. Note also that, in this case, the spacecraft was considered to have $\beta = \beta_0$ during the whole mission and the value of $\Delta\beta$ is added at the end-of-life, so $\beta = \beta_0 + \Delta\beta$. In order to make our results comparable with the work by Olikara et al.,[2] we introduced the concept of the equivalent Δv_{eq} provided by SRP.

Equivalent Δv_{eq}

The equivalent Δv_{eq} quantifies how much theoretical Δv is needed for a traditional propulsion system to augment the energy of the spacecraft to achieve the same energy level allowed by the use of a reflective SRP enhancing device. Note that, it cannot be effectively achieved by a propulsion system since the effect of SRP changes the shape of the potential which is not possible with a traditional propulsion-based approach. Set $E_0 = E(x_0, y_0, z_0, \dot{x}_0, \dot{y}_0, \dot{z}_0, \beta_0)$ (see Eq. (13)) as the initial energy of the system before the deployment and E_{SL_2} as the energy of the system after the deployment.

$$E_{SL_2} = \frac{1}{2}V^2 - \frac{1}{2}(x_0^2 + y_0^2) - \frac{\mu_{Sun}}{r_{Sun-p}} - \frac{\mu_{Earth}}{r_{Earth-p}} + \beta_0 \frac{\mu_{Sun}}{r_{Sun-p}} + \Delta\beta \frac{\mu_{Sun}}{r_{Sun-p}} \tag{23}$$

Now let's make the hypothesis that E_{SL_2} is achieved with a traditional propulsion system; therefore we can write:

$$E_{SL_2} = \frac{1}{2}V_{new}^2 - \frac{1}{2}(x_0^2 + y_0^2) - \frac{\mu_{Sun}}{r_{Sun-p}} - \frac{\mu_{Earth}}{r_{Earth-p}} + \beta_0 \frac{\mu_{Sun}}{r_{Sun-p}} \tag{24}$$

Therefore, the velocity required is:

$$\frac{1}{2}V_{new}^2 = E_{SL_2} + \frac{1}{2}(x_0^2 + y_0^2) + \frac{\mu_{Sun}}{r_{Sun-p}} + \frac{\mu_{Earth}}{r_{Earth-p}} - \beta_0 \frac{\mu_{Sun}}{r_{Sun-p}} \tag{25}$$

By adding Eq. (23) to Eq. (25) and simplifying, we get:

$$\frac{1}{2}V_{new}^2 = \frac{1}{2}V^2 + U_s(x_0, y_0, z_0, \Delta\beta) \tag{26}$$

From where the equivalent Δv_{eq} can be derived as:

$$\Delta v_{eq} = V_{new} - V = \sqrt{V^2 + 2\Delta\beta \frac{\mu_{Sun}}{r_{Sun-p}}} - V \tag{27}$$

HERSCHEL

Herschel was lunched in 2009 and its mission objectives were to study the stars and galaxies formations. At the EOL, Herschel was placed in a halo orbit around L_2 with a period of 180 days. For the disposal, 40 trajectories equally distributed along the halo were selected. The time step along the halo was set to 4.6 days; where, the initial condition along the halo is on the farther side from the Sun. Each single unstable trajectory is obtained by integrating forward in time for 6 years. The time step selected along the trajectory leg is 0.05 in non-dimension units, which, correspond to 2.89 days. Figure 9a shows the area-to-mass requirement as a function of the curvilinear coordinate on the LPO (y-axis) and the time along the trajectory leg (x-axis). The minimum required area-to-mass ratio is 0.266 m^2/kg and the maximum ratio is 38.52 m^2/kg. The correspondent β_{min} is 4.06 $\cdot 10^{-4}$ and the β_{max} is 0.059. The initial β used is the one of Herschel of $7.803 \cdot 10^{-6}$ which correspond to an area-to-mass dry of 0.0051 m^2/kg. Figure 9b shows the magnitude of the Δv_{eq} due to the effect of the increasing energy of the system after the deployment. The spaceraft-Sun distance and the initial solar radiation pressure acceleration of Herschel are represented in Figure 10 as a function of the curvilinear coordinate on the halo during six years of disposal. This also shows that the peaks are due to the fact that, along one trajectory, the spacecraft motion oscillates around the Hill's curves. The dry mass of Herschel is 3144 kg; therefore, the minimum overall area required for the disposal is of 836.304 m^2. The initial reflective area for Herschel is around 16 m^2 from the solar panels and sunshade. Therefore, the minimum delta area needed at the EOL is 820.304 m^2 (28.64 m span for a squared flap or additional EOL device) to close the zero velocity curves with SRP for Herschel.

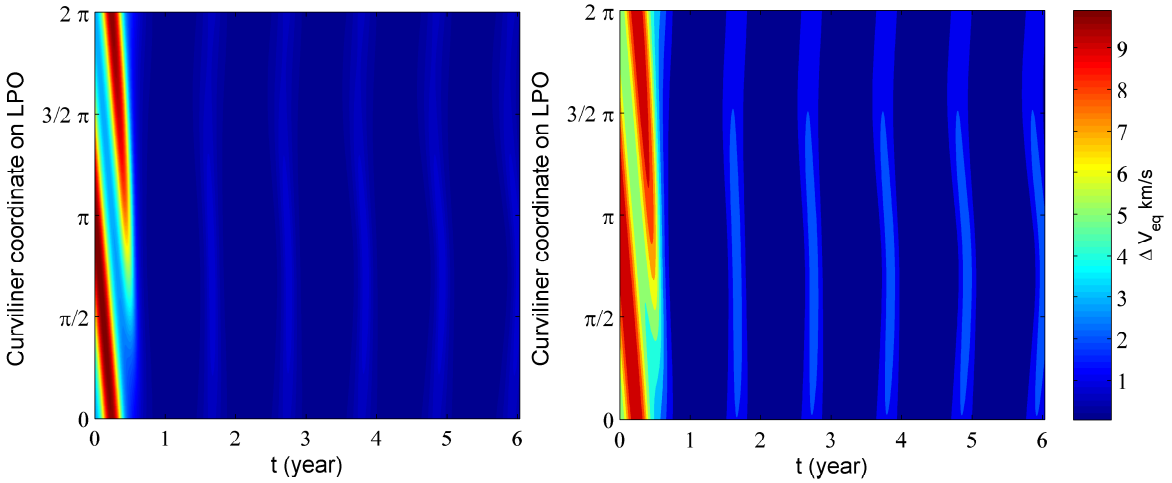

(a) Herschel area-to-mass ratio for disposal within six years.

(b) Herschel Δv_{eq} for the closure in SL_2 within six years.

Figure 9: Herschel area-to-mass ratio and equivalent Δv_{eq}.

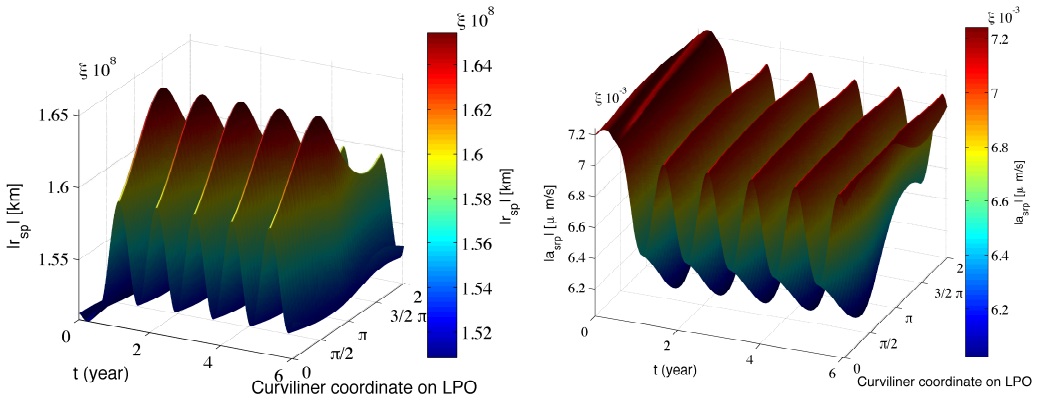

(a) (b)

Figure 10: Distance from the Sun and SRP acceleration for Herschel $A/M_{dry} = 0.0051$ m^2/kg.

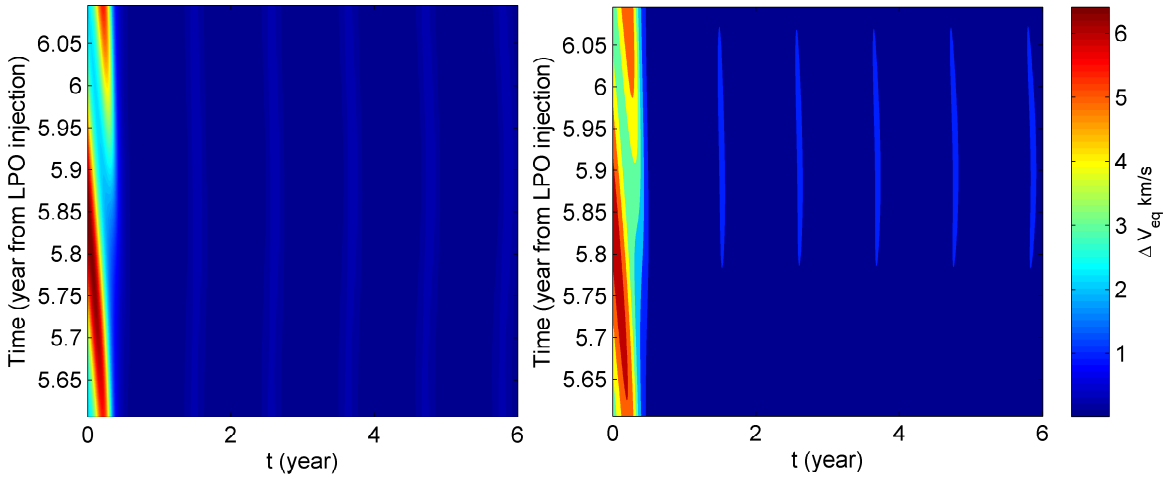

(a) Gaia area-to-mass ratio for disposal within six years .

(b) Gaia Δv_{eq} for the closure in SL_2 within six years.

Figure 11: Gaia area-to-mass ratio and equivalent Δv_{eq}.

GAIA

Gaia was recently placed in a Lissajous orbit around L_2 and its mission objective is to provide a 3D map of our galaxy. For the EOL analysis, several trajectories were selected along the Lissajous orbit, from 5.59 to 6.1 years since the start of the mission; each initial injection corresponds to Gaia crossing the x-z plane. Each unstable trajectory is obtained by integrating forward in time until 6 year. The time step selected along the trajectory leg is of 0.05 in non-dimensional unit, which, corresponds to 2.89 days. Figure 11a represents the required area-to-mass ratio at the EOL. With respect to Herschel, the maximum area required is lower since Gaia has a lower total mass than Herschel. Consequently, the trend in the equivalent Δv_{eq} is lower as well for Gaia rather than for the Herschel case (see Figure 11b). The minimum required area-to-mass ratio is 0.135 m^2/kg and the maximum ratio is 15.98 m^2/kg (this area-to-mass range is approximately half of the Herschel area-to-mass range). The correspondent β_{min} is 2.1 $\cdot 10^{-4}$ and the β_{max} is 0.02446. The initial β for Gaia is of $8.98 \cdot 10^{-5}$ which correspond to a dry area-to-mass of 0.059 m^2/kg. In Figure 12, the spaceraft-Sun distance and the initial solar radiation pressure of Gaia has been computed when considering its dry area-to-mass as a function of the curvilinear coordinate on the halo during six years of disposal. As in the case of Herschel, it can be noticed that the peaks are due to the fact that along one trajectory the spacecraft motion oscillates around the Hill's curves. The dry mass of Gaia is 1392 kg; therefore, the minimum overall area required is around 187.92 m^2. The initial reflective area of Gaia is 69 m^2 of sunshade; therefore, the deployable delta area required is 118.92 m^2 (10.9 m span for a squared flap or additional EOL device).

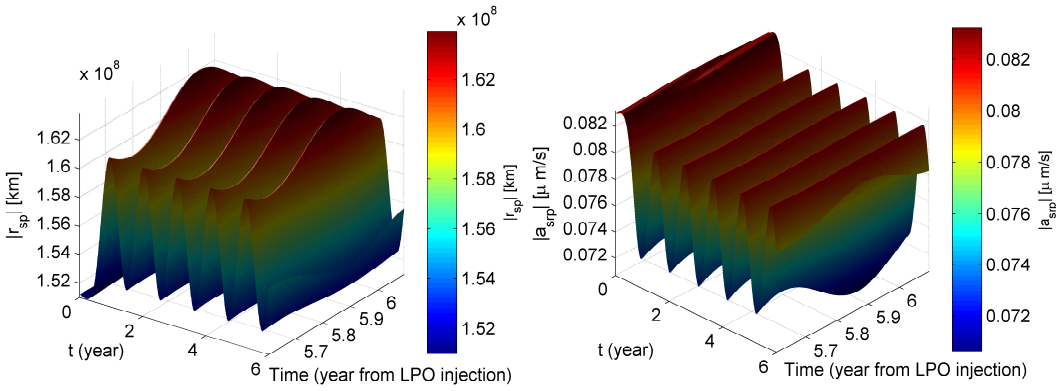

(a) (b)

Figure 12: Distance from the Sun and SRP acceleration for Gaia $A/M_{dry} = 0.059$ m^2/kg.

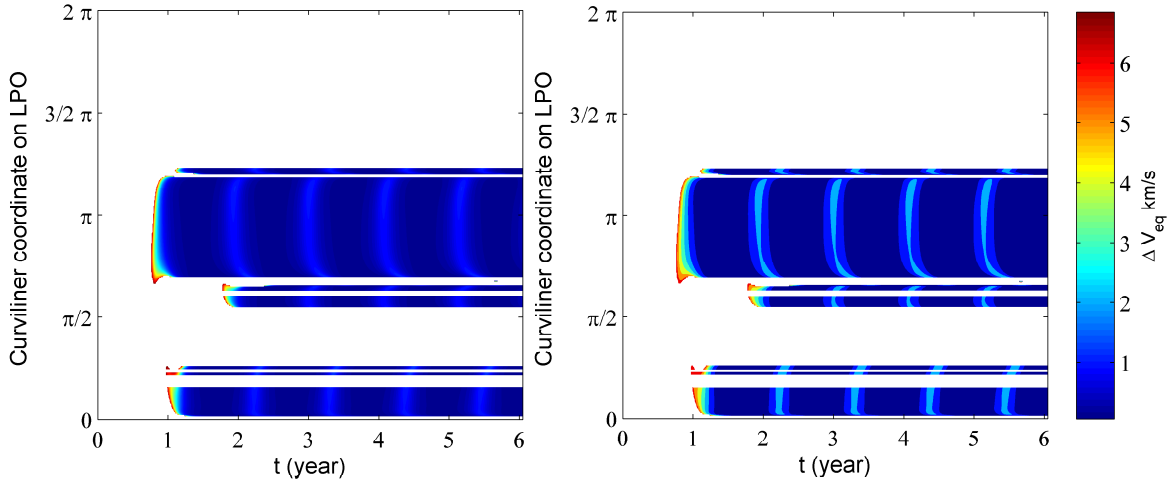

(a) SOHO area-to-mass ratio for disposal within six years.

(b) SOHO Δv_{eq} for the closure in SL_2 within six years.

Figure 13: SOHO area-to-mass ratio and equivalent Δv_{eq}.

SOHO

SOHO was lunched in 1995 and it was placed in a halo orbit with a period of 178 days around L_1, therefore the closure of the zero velocity curves in SL_2 should be done more carefully than in the case of Herschel and Gaia. After the injection from the halo to the unstable tube towards the outer system, the disposal was investigated up to 6 years from the moment of injection. In the case of SOHO, it is necessary to control the Earth passage of these trajectories. First of all, trajectories that pass below 60,000 km from the centre of the Earth were excluded, since it is unsafe to transfer below of this region. Moreover, the trajectories above 60,000 km belongs to two families: one orbit family after the Earth passage comes back to L_1 and moves towards the inner planets; the second family, instead, after passing by the Earth, transfers through L_2 and moves towards the outer system. Therefore, it has been verified that the spacecraft follows a trajectory towards the outer system. Figure 13a shows, as for Herschel and Gaia, the trend in the area-to-mass ratio required at the EOL. In term of the results, SOHO is a satellite with a similar mass magnitude as Gaia. Since SOHO is placed in halo around L_1, it is interesting to notice that the disposal is not always possible when compared with Herschel and Gaia cases. Indeed, it is possible to note that the white strips correspond to two class of trajectories: the one that goes bellow 60,000 km from Earth and the one that never pass by the gateway in L_2 (after several revolutions around the Earth, this trajectory goes back towards the Sun). Moreover, the coloured stripes shows when the spacecraft crosses the L_2 gateway; therefore, some unstable trajectories can spend several years crossing around the Earth region and reach L_2, for example, after two years, which is not really a fast and efficient disposal solution. The range of values in the area-to-mass ratio and in the Δv_{eq} for SOHO are an average of the Herschel and Gaia cases (see Figure 13). The minimum required area-to-mass ratio is 0.28 m^2/kg and the maximum ratio is 18.08 m^2/kg. The correspondent β_{min} is 4.35 $\cdot 10^{-4}$ and the β_{max} is 0.028. The initial β for SOHO is of $3.2 \cdot 10^{-5}$, which corresponds to a dry area-to-mass of 0.021 m^2/kg. In Figure 14, the spacecraft-Sun distance and the initial solar radiation pressure of SOHO when considering its dry area-to-mass as a function of the curvilinear coordinate on the halo during six years of disposal has been computed. Again, the peaks are due to the fact that along one trajectory the spacecraft motion oscillates around the Hill's curves. The dry mass of SOHO is 1602 kg; therefore, the minimum overall area required is around 448.56 m^2. The initial reflective area of SOHO is of 22 m^2 in the solar panels; therefore, the deployable delta area required is 426.56 m^2 (20.65 m span for a squared flap or additional EOL device).

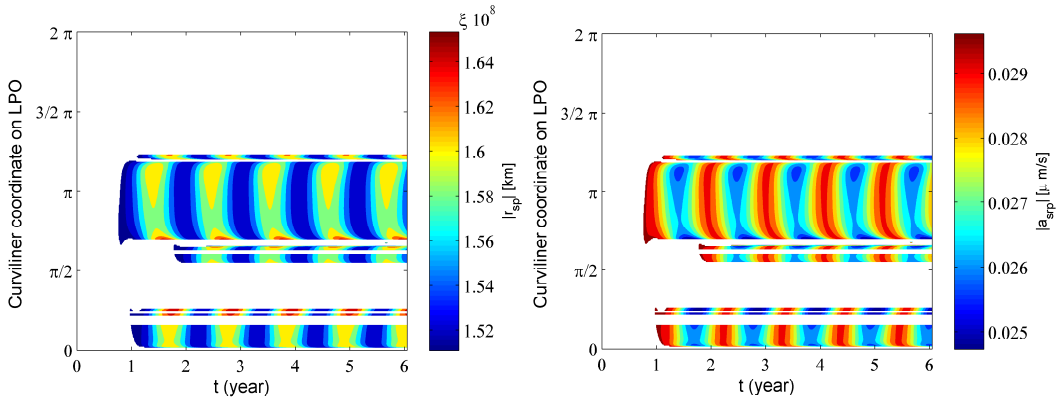

(a) (b)

Figure 14: Distance from the Sun and SRP acceleration for SOHO $A/M_{dry} = 0.021$ m^2/kg.

DISCUSSION

The main features of the disposal strategy by means of solar radiation pressure for the zero velocity curves closure are that the device should be constrained to be sun-pointing, thus a self-stabilised deployable structure is required. When compared to a strategy using traditional propulsion methods, the disposal throughout SRP can be achieved to close the zero velocity curves around SL_2 (it can not be achieved the condition of closing the curves in SL_1 and dispose the spacecraft towards the Sun). It should be also taken into account that to inject the spacecraft onto the unstable manifold a small Δv manoeuvre is required. Since the acceleration of SRP is a function of the inverse square of the Sun-spacecraft distance, the minimum required area for the disposal is lower if the deployment is done far away from the Sun. Thus, SL_2 is much closer to L_2. Therefore, it is possible to better protect the L_2 region. Note that, the majority part of the halo orbit is protected from spacecraft impact hazards because of the closure of the gateway trajectories throughout L_2. In a case where the energy associated to the spacecraft initial orbit is higher, a higher area is required to perform the closure of the zero velocity curves at the same distance from the Sun.

CONCLUSION AND FUTURE WORK

This paper investigates an end-of-life strategy which uses a solar radiation enhancing deployable device to close the zero velocity curves at the pseudo Lagrangian point SL_2 preventing the spacecraft's Earth return. The simulations have focused on studying the motion of the spacecraft after the deployment of a device at one location along the unstable manifold. The effect of SRP does not affect the overall final results in term of area required; however, the comparison of the unstable manifolds computed with and without the effect of SRP show that the positions along the manifolds are slightly shifted. Therefore, if the SRP is not taken into account after the injection its effect can add an uncertainty on when the deployments should be performed. This study was verified for three ESA missions: Herschel, Gaia and SOHO when SRP is included after the manifold injection. Those spacecraft are placed respectively in a halo orbit, a Lissajous orbit around L_2 and in a halo orbit around L_1. It has been demonstrated that, after the injection into the unstable manifold, it is not always possible to close the Hill's curves, for example, for a spacecraft around L_1 such as SOHO (white strip solutions Figure 13). The minimum required delta area in the CRTBPS is around 28 m-span for Herschel, 21 m-span for SOHO and 11 m-span for Gaia. An additional EOL device for Herschel and Gaia missions cannot be easily achieved with additional flaps since their current sunshade configuration in term of shape does not allow the deployment of flaps. Instead, SOHO can potentially support additional solar panel flaps; however, the area provided by the solar panel is too small to support 20-m span of flaps (e.g., solar concentrator). Note that JAXA has recently demonstrated the capability to deploy a 20 m-span sail with the Ikaros mission.[16] Therefore, the disposal of Herschel seems to be the worst case to achieve with a SRP enhancing device due to its 28 m-span required. However, spacecraft with the same characteristics in terms

of configurations and masses such as Herschel, Gaia and SOHO, will require an specifically designed EOL stabilising deployable sail like the one used for attitude control (e.g., GOES mission[3]) or the one proposed by Ceriotti et al.[9] In the cases studied, the EOL delta area is on the order of 20 m-span and it will cover the spacecraft bus when deployed. Thus, the contribution of the sunshade or solar array is neglected and it is no longer possible to design the EOL device with delta area but it should be used the total area required (for example if the spacecraft's sunshade is covered by the EOL device, the EOL area should be bigger enough to include the shaded sunshade area). This study shows that, if it will be possible to take into account the EOL as part of the mission design, it would be possible to include additional flaps for the disposal. Furthermore, an area margin should be included to counteract the effect of perturbations in the full body system. Therefore, an analysis is currently being performed in the ERTBP[6] to verify the effect of the Earth's eccentricity on the disposal strategy and to possibly quantify the area margin that should be included. However, Olikara et al.[2] already proved that the overall return trajectories to the Earth in the CRTBP and in the full-body (ephemeris) are quite similar; therefore, the CRTBP seems a good approximation of the spacecraft's dynamics. Finally, further studies will include the reflectivity distribution of the spacecraft's component by defining an equivalent reflectivity coefficient for a precise EOL disposal area design *.

ACKNOWLEDGEMENT

The authors would like to acknowledge Dr. Elisa Maria Alessi from SpaceDyS for providing the initial conditions for the orbits of Herschel, SOHO and Gaia spacecraft. Moreover, S. Soldini would like to acknowledge the Institution of Engineering and Technology for providing a travel financial support to attend the IAA-AAS-DyCoSS2. C. Colombo acknowledges the support received by the Marie Curie grant 302270 (SpaceDebECM - Space Debris Evolution, Collision risk, and Mitigation).

REFERENCES

1 C. Colombo, H. Lewis, F. Letizia, S. Soldini, L. Gössnitzer, E. M. Alessi, A. Rossi, L. Dimare, M. Vasile, W. V. D. Weg, C. McInnes, M. Macdonalds, and M. Landgraf, "End-of-Life disposal trajectories for libration point and highly elliptical orbit missions," *Proceedings of the* 64^{th} *International Astronautical Congress*, IAC-13.A6.P.24, Beijing, China, 23-27 September, 2013.

2 Z. Olikara, G. Goméz, and J. J. Masdemont, "End-of-life disposal of libration point orbit spacecraft," *Proceedings of the* 64^{th} *International Astronautical Congress*, IAC-13.C1.82., Beijing, China, 23-27 September, 2013.

3 DRL-101-08, *GOES I-M DataBook*. Contract NAS5-29500, 1996.

4 A. I. S. McInnes, *Strategies for solar sail mission design in the circular restricted three-body problem*. Master of science in engineering, 2000.

5 C. R. McInnes, *Solar sailing: technology, dynamics and mission applications*. Glasgow, Scotland: Springer, 1998.

6 V. Szebehely and G. E. O. Giacaglia, "On the elliptic restricted three body problem," *The Astronomical Journal*, Vol. 69, No. 3, 1964, pp. 230–235.

7 H. Baoyin and C. R. McInnes, "Solar sail equilibria in the elliptical restricted three-body problem," *Journal of Guidance, Control and Dynamics*, Vol. 29, No. 3, 2006, pp. 538–543.

8 V. Szebehely, *Theory of orbits in the restricted problem of three bodies*. New York: Academic Press Inc., 1967.

9 M. Ceriotti, P. Harkness, and M. McRobb, "Variable-geometry solar sailing: the possibility of the quasi-rhombic pyramid," *3rd International Simposyum on Solar Sailing 2012 (ISSS 2013)*.

10 Z. M. F. Szenkovits and I. Csillik, "Polynomial representation of the zero velocity surfaces in the spatial elliptic restricted three-body problem," *Pure Mathematics and Application*, Vol. 15, No. 2-3, 2004, pp. 323–322.

11 J. E. M. Wang Sang Koon, Martin W. Lo and S. D. Ross, *Dynamical systems, the three-body problem and space mission design*. Marsden Books, ISBN 978-0-615-24095-4, 2008.

*In Eq. (7), C_r was already considered equal to 2 so it is not explicitly present in this equation. The SRP accelerations for a Sun-pointing area can be therefore expressed as: $\boldsymbol{a}_s = -\beta \frac{C_r}{2} \frac{\mu_{Sun}}{r^3_{Sun-p}} \boldsymbol{r}_{Sun-p}$. In this last equation, can be replaced the area A with the overall spacecraft area illuminated by the Sun A_t and the C_r with an equivalent coefficient which weights the different spacecraft's reflectivity surfaces C_r^* which will take into account the real spacecraft's reflectivity distribution.

12 J. M. G. Goméz, Á. Jorba and C. Simó, *Dynamics and mission design near libration points: advanced methods for collinear points v. 3*. World Scientific Monograph Series in Mathematics, 1991.

13 R. Bauske, "Operational manoeuvre optimization for the ESA missions Herschel and Planck," *International Symposium on Space Flight Dynamics*, 2009.

14 F. B. Olive J. P., Overbeek T. V., "SOHO monthly trending report," *Ref. SOHO/PRG/TR/769 Oct 15*, 2013.

15 M. M. E. Canalias, G. Goméz and J. J. Masdemont, "Assessment of Mission Design Including Utilization of Libration Points and Weak Stability Boundaries," *Ref. ESA Advanced Concepts Team Ariadna id: 03/4103*, 2008.

16 Y. Tsuda, O. Mori, R. Funase, H. Sawada, T. Yamamoto, T. Saiki, T. Endo, K. Yonekura, H. Hoshino, and J. Kawaguchi, "Achievement of IKAROS Japanese deep space solar sail demonstration mission," *Acta Astronautica*, Vol. 82, Feb. 2013, pp. 183–188, doi: 10.1016/j.actaastro.2012.03.032.